Novel hydroxyapatite/carboxymethylchitosan composite scaffolds prepared through an innovative "autocatalytic" electroless coprecipitation route

J. M. Oliveira,[1,2] S. A. Costa,[1,2*] I. B. Leonor,[1,2] P. B. Malafaya,[1,2] J. F. Mano,[1,2] R. L. Reis[1,2]
[1]*3B's Research Group - Biomaterials, Biodegradables and Biomimetics, Department of Polymer Engineering, University of Minho, Campus de Gualtar, 4710-057 Braga, Portugal*
[2]*IBB - Institute for Biotechnology and Bioengineering, PT Government Associated Laboratory, Braga, Portugal*

Received 31 May 2007; revised 26 September 2007; accepted 15 October 2007
Published online 27 February 2008 in Wiley InterScience (www.interscience.wiley.com). DOI: 10.1002/jbm.a.31817

Abstract: A developmental composite scaffold for bone tissue engineering applications composed of hydroxyapatite (HA) and carboxymethylchitosan (CMC) was obtained using a coprecipitation method, which is based on the "autocatalytic" electroless deposition route. The results revealed that the pores of the scaffold were regular, interconnected, and possess a size in the range of 20–500 μm. Furthermore, the Fourier transform infra-red spectrum of the composite scaffolds exhibited all the characteristic peaks of apatite, and the appearance of typical bands from CMC, thus showing that coprecipitation of both organic and inorganic phases was effective. The X-ray diffraction pattern of composite scaffolds demonstrated that calcium-phosphates consisted of crystalline HA. From microcomputed tomography analysis, it was possible to determine that composite scaffolds possess a 58.9% ± 6% of porosity. The 2D morphometric analysis demonstrated that on average the scaffolds consisted of 24% HA and 76% CMC. The mechanical properties were assessed using compressive tests, both in dry and wet states. Additionally, *in vitro* tests were carried out to evaluate the water-uptake capability, weight loss, and bioactive behavior of the composite scaffolds. The novel hydroxyapatite/carboxymethylchitosan composite scaffolds showed promise whenever degradability and bioactivity are simultaneously desired, as in the case of bone tissue-engineering scaffolding applications. © 2008 Wiley Periodicals, Inc. J Biomed Mater Res 88A: 470–480, 2009

Key words: hydroxyapatite; carboxymethylchitosan; composite scaffolds; biodegradable; tissue engineering; coprecipitation method; wax spheres leaching methodology; "autocatalytic" electroless bath

INTRODUCTION

The innovative tissue engineering (TE) concept promises the creation of viable substitutes for the repair, replacement, or regeneration of organs and tissues, allowing a wide range of novel therapeutical possibilities.[1] This area of expertise deals with three main strategies: (i) combining of living cells with specially designed biomaterials,[2,3] (ii) use of cells isolated or cell substitutes,[4–6] and (iii) targeted-delivery of bioactive molecules, such as growth and differentiation factors by using drug-delivery carriers.[7–9]

Scaffold technologies play a central role in the field of TE, since the main aim of the scaffold is to act as a support and guidance template for the development of a new tissue, both *in vitro* and *in vivo*.[10] Therefore, the size of the channels or pores as well as the 3D architecture has a great effect on the cell seeding, infiltration, and consequently on the tissue regeneration.[11–13] For instance, when engineering bone tissue, the scaffolds should meet these important criteria. It must be biocompatible,[14] biodegradable in an appropriate time window, its degradation products should be nontoxic and easily eliminated by the metabolic pathways, it should

**Present address:* EACH-Escola de Artes, Ciências e Humanidades, Curso de Tecnologia Têxtil, Universidade de São Paulo, Campus USP-Leste, Av. Arlindo Bétio, 1000 – Parque Ecológico do Tietê – Ermelino Matarazzo, 03828-080 São Paulo – S.P., Brasil
Correspondence to: J. M. Oliveira; e-mail: miguel.oliveira@dep.uminho.pt
Contract grant sponsor: Foundation for Science and Technology (FCT) (POCTI and/or FEDER programmes); contract grant numbers: SFRH/BD/9031/2002, SFRH/BPD/8469/2002, SFRH/BD/11155/2002, SFRH/BD/21786/2005
Contract grant sponsor: European Union (STREP Project HIPPOCRATES); contract grant number: NMP3-CT-2003-505758

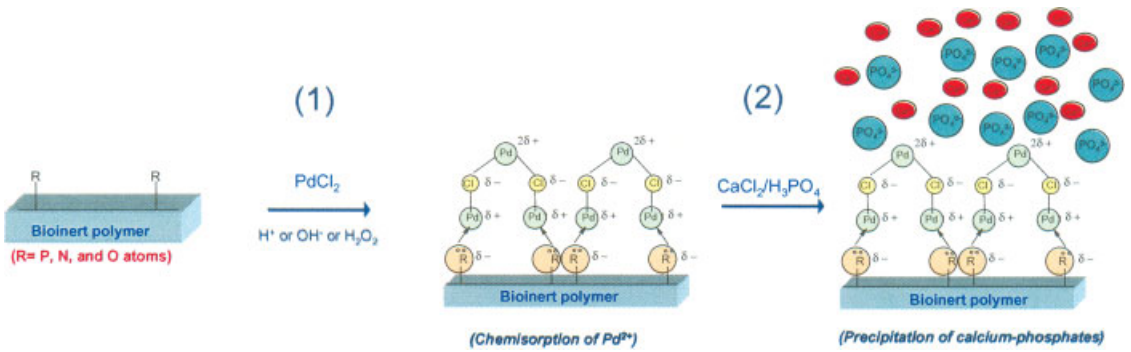

Figure 1. Schematic representation of the autocatalytic electroless route to modify the surface of bioinert and biodegradable polymers with calcium-phosphates. [Color figure can be viewed in the online issue, which is available at www.interscience.wiley.com.]

support cell adhesion and growth, and possess adequate mechanical stability.[1,10,15–18] The material should induce bone formation (osteoinductive) in addition to allow new bone ingrowths (osteoconductive),[19] while facilitating the angiogenesis[1,10] to supply the newly formed tissue with nutrients.

In recent years, great efforts have been made toward the development of new synthetic skeletal substitute products.[20–22] Among these, bioceramics and polymeric scaffolds have attracted much attention, for example hydroxyapatite (HA, $Ca_{10}(PO_4)_6(OH)_2$)[23,24] and chitosan,[25,26] respectively. Since there is not yet a single material that fulfils all the necessary requirements for bone TE scaffolds,[27] composites have been developed.[27–34] Mechanical properties are one of the great advantages of composites, as they usually show a good balance between strength and toughness,[17] and their improved osteoconductivity and biodegradability are also of interest.[33] From this point of view, composites materials are a better choice for such type of applications.[35,18] Bearing these assumptions in mind, Reis and coworkers focused their efforts on creating innovative TE composite scaffolds based on natural-derived polymers and ceramics.[36]

Carboxymethylchitosan (CMC) is a biocompatible and biodegradable chitin or chitosan-derivative polymer.[37] There are several types of carboxymethylated chitosans which can be prepared through different methods.[38,39] Of particular interest is the fact that unlike chitin and chitosan, CMC is a water-soluble polymer.[38,40] Its versatility allowed many applications, such as metal ion chelating agents,[40,41] drug delivery,[42,43] and medicine.[44]

Muzzarelli[38] reported that chitosan does not bind significantly with calcium ions. On the contrary, CMC adsorb calcium ions to an extent that is dependent on proportion of protonation or if the molecule is in salt form of sodium. In this report, an important peculiarity of CMC was demonstrated. By attracting the calcium ions it is expected that it can have an effect on the precipitation of biominerals,[45] or on the growth of the crystals either *in vitro* or *in vivo*.[46,47]

Here we report a coprecipitation route for the preparation of hydroxyapatite/carboxymethylchitosan (HA/CMC) composite materials. This method is based on a previously reported "autocatalytic" electroless bath[48,49] that has been used in our group to modify the surface of bioinert and biodegradable polymers (Fig. 1).[49] This methodology is based on the possibility of chemisorption of Palladium (Pd^{2+}) on the surface of bioinert polymers (1), which acts as the catalyst to induce the precipitation of calcium-phosphate on its surface (2).[50–53] Since it is known that CMC is able to chelate metal ions,[40] we expect CMC to bind Pd^{2+}. As illustrated in Figure 1 the resulting excess of positive charge from the CMC/Pd^{2+} complex may build up an adjacent layer of negative charges (phosphate groups), which can create a residual charge responsible for attracting other calcium ions. Consequently, calcium phosphate precipitation may occur in the presence of CMC because of a local supersaturation followed by calcium phosphate nucleation.[32] In this context, we hypothesized that by using an acidic autocatalytic electroless bath it may be possible to create the coprecipitation of calcium-phosphates and CMC.

As previously highlighted the porosity of scaffolds greatly dictates the performance of a 3D template in the TE approaches. Therefore, the development of novel processing routes toward the fabrication of adequate porous structures is of great interest. The novelty of this work consists of the possibility of tailoring the porosity and 3D architecture of the composite materials by using a wax spheres leaching method. The physicochemical characterization of composite scaffolds was performed by X-ray diffraction (XRD) analysis, Fourier transform infra-red spectroscopy, microcomputed tomography, and scanning electron microscopy attached with an X-ray

detector. Complementarily, mechanical properties of composite scaffolds were determined under compression testing, in dry and wet states.

In vitro tests were carried out to assess the swelling and weight loss behavior. The bioactive character of the composite scaffolds was also investigated by means of soaking the composite scaffolds in a simulated body fluid (SBF) solution. The elemental composition in the SBF solution was monitored by inductively-coupled plasma optical emission spectrometry.

MATERIALS AND METHODS

Materials

Reagent grade chitosan particles with a deacetylation degree of ~91% and size in the range of 125–250 μm (Vanson, USA), monochloroacetic acid (Sigma, USA), acetic acid (Fluka, Switzerland), sodium hydroxide 40% (Merck, Germany) solution, and acetone (Pronalab, Portugal) were used in the preparation of CMC.

Calcium chloride, $CaCl_2$ (Merck, Germany); ortho-phosphoric acid, H_3PO_4 (Panreac, Spain); and palladium chloride, $PdCl_2$ (Aldrich, USA) were used to prepare the acidic autocatalytic electroless bath, and ammonium hydroxide 33%, NH_4OH (Riedel-de Haën, Germany) solution to adjust the pH of the coprecipitation media.

Hydration and weight loss tests were performed using phosphate-buffered saline (PBS) tablets supplied by Sigma (Sigma-Aldrich, Germany).

The SBF solution was prepared as previously reported by Kokubo et al.[54]

Potassium bromide, KBr (Riedel-de Haën, Germany) suitable for spectroscopy was used to prepare the FTIR pellets.

Preparation of the composite scaffolds

CMC was prepared by a modification of the reaction process previously reported by Chen and Park.[55] The composite materials were prepared by a coprecipitation method using an acidic autocatalytic electroless bath.[48] The acidic electroless bath was prepared by dissolving calcium chloride with a final concentration of 5.6 g L^{-1}, orthophosphoric acid 3.4 g L^{-1}, and palladium chloride 0.9 g L^{-1} in 500 mL distilled water, under agitation. A 10 wt % CMC aqueous solution was added to the bath using a peristaltic pump (Gilson Miniplus 3, France) at a speed rate 2 mL min^{-1}. The composite precipitate was obtained by means of adjusting the pH of the bath to 6 with ammonium hydroxide. The precipitate was filtered under vacuum and the excess water removed by drying at 37°C for 24 hours. Porous structures were prepared by mixing the composite filtrate and 20 wt % wax spheres (Desert Whale Jojoba Company, USA), with a diameter ranging from 50 to 450 μm, and transferring into a cylindrical mold with 4–7 mm diameter and 8–22 mm height. After drying at 60°C, the wax spheres were eliminated by soaking in tetrahydrofuran (Riedel-de Haën, Germany), in an ultrasound bath, for several hours. Composite scaffolds were allowed to dry until constant weight and the scaffolds were frozen at −80°C overnight, followed by freeze-drying for a period of 2 days to completely remove the organic solvent.

Swelling and weight loss studies

Water-uptake or swelling and weight loss of the developed composite scaffolds were performed, by soaking in a PBS solution for up to 30 days, in triplicate. The solution was prepared by dissolving 1 tablet of PBS in 200 mL of distilled water to obtain a final concentration of 0.0027*M* potassium chloride and 0.137*M* sodium chloride, pH 7.4 at 25°C. The water-uptake was determined by the changes on the initial mass of the scaffolds (m_i) after incubation in the PBS solution at 37°C ± 1°C. The scaffolds were removed after 1, 3, 7, 15, 21, and 30 days of immersion, the excess solution removed with a filter paper, and the mass (m_w) was determined using an analytical balance. Then, scaffolds were dried at 60°C until constant weight. The mass is determined (m_d) in order to obtain the weight loss. The percentage of water-uptake of scaffolds (WUs) after each time of immersion (t) was calculated by

$$WU_{s,t} = [(m_{w,t} - m_i)/m_i] \times 100 \quad (1)$$

The percentage of weight loss of the scaffolds (WLs) after each immersion (t) was calculated using

$$WL_{s,t} = [(m_{d,t} - m_i)/m_i] \times 100 \quad (2)$$

Bioactivity test

Bioactivity tests were performed by soaking the scaffolds in a SBF solution at 37°C ± 1°C for a period of time ranging from 1 to 30 days. This solution contained inorganic ion concentrations resembling those found in human blood plasma and pH of 7.4.[54] After each soaking time, the scaffolds were removed from the SBF solution and immediately rinsed with distilled water, dried at room temperature for 24 hours and in the oven at 60°C until constant weight. The concentration of the Ca and P ions, after each soaking time, was measured by inductively-coupled plasma optical emission (ICP-OES, JY 70 plus, JobinYvon, France) spectrometry. Triplicate samples were analyzed for each soaking time and an average result was calculated.

Mechanical properties

Compression tests in dry state were performed using a Universal Testing Machine (Instron 4505) possessing a load cell of 50 kN. A minimum number of 10 composite scaffolds were tested after storage at ~20°C and 55% relative humidity, to obtain an average result. Tests were conducted up to failure or until 60% reduction in specimen height was reached as previously reported by Boesel et al.[56] Compression tests "Push-out" in wet state were carried out by using a Miniature Materials Tester (Minimat Vsn 3.1,

Rheometric Scientific, UK). This equipment is capable of sensing full scale load ranges from 20 N up to 1000 N at 37°C. Before conducting the tests, composite scaffolds were introduced inside the perforated stainless steel shells (6 mm of diameter and 11 mm height), and soaked in a PBS solution for 24 hours at 37°C inside an oven. Afterward, the shells containing the composite scaffolds were immersed in a PBS solution at 37°C and a minimum number of 5 samples were tested. A baseline was also performed for each sample using the same experimental conditions but running the experiments with the empty stainless steel shells.

Scanning electron microscopy

The microstructure of the composite scaffolds before and after immersion into the SBF solution was determined by using a scanning electron microscope, SEM (Leica Cambridge S-360, UK). Prior to the elemental and microstructure analysis, specimens were coated with carbon (Fisons Instruments, Polaron SC 508, UK) and gold (Fisons Instruments, Polaron SC 502, UK), respectively. The current was set at 18 mA with a coating time of 120 seconds. The phosphorus, calcium, sodium, carbon, and oxygen elemental analysis was achieved by means of using an X-ray detector, EDS (Pentafet model 5526, UK) attached to the S-360 microscope, and a voltage of 10 keV was used.

Fourier transform infra-red spectroscopy

Fourier transform infra-red (FTIR) analysis was performed using a Perkin-Elmer spectroscope (Perkin-Elmer 1600 series equipment). Transparent KBr pellets were prepared by mixing in the ratio of 1:10 of sample/KBr (w/w), and milling in an agate mortar, followed by uniaxially pressing the powders. All transmission spectra were recorded in the region of 4400–450 cm^{-1}, using a minimum of 32 scans, and a 2 cm^{-1} resolution.

X-ray diffraction

X-ray diffraction (XRD) analysis was performed on powder samples of CMC and composite scaffolds, using an X-ray diffractometer with Cu Kα radiation at 50 mA and 40 kV (Philips PW 1710, The Netherlands). Using flat plate geometry, data were collected from 2° to 62° 2θ values, with a step size of 0.02°, and a counting time of 2 seconds.

Microcomputed tomography

Microcomputed tomography (μ-CT) of the composite scaffolds was carried out using a Scanco 20 equipment (Scanco Medicals, Switzerland). Mimics® from Materialise (Belgium) was used as image processing software. The X-ray scans were performed in high resolution mode (9 μm) and 240 slices of the material were obtained. The 2D morphometric analysis of the scaffolds was performed using a threshold 51 to identify the polymeric phase to determine the porosity, and a threshold 133 to identify the HA content along the scaffold (from 0 to 2000 μm).

RESULTS

Figure 2 shows the SEM morphology and EDS analysis of the composite scaffolds. These results revealed that the pores of the scaffolds were regular with sizes in the range of 20–500 μm [Fig. 2(A)]. Additionally, it is possible to observe a typical interconnected macropores in sizes greater than 200 μm [Fig. 2(B)]. At high magnification, it is possible to observe that CMC (white arrow) coprecipitated with ceramic particles (black arrow) [Fig. 2(C)], and that these particles were homogeneously distributed throughout the polymer network. The EDS analysis corroborated previous studies showing that particles are calcium and phosphate in nature [Fig. 2(D)].

The FTIR spectra of chitosan and CMC demonstrated that the latter was successfully synthesized, as detected by the presence of characteristic absorption bands of the carboxyl group (□) at 1593 and 1417 cm^{-1} (υas COO^- and υs COO^-) [Fig. 3(A,B)]. The FTIR spectrum of the composite scaffolds revealed the presence of two types of phosphate absorption bands, PO_4^{3-} (ν3) at 1190–1020 cm^{-1} (+), and the PO_4^{3-} (ν4) bands at 601 and 565 cm^{-1} (×) [Fig. 3(C)]. It also detected the presence of the peaks corresponding to the carbonate groups, namely at 875 cm^{-1} attributed to carbonate ν2 (*) and at 1650–1300 cm^{-1} assigned to carbonate ν3 (●), which can be indicative of the carbonate ion substitution. The appearance of a band (□) at 1417 cm^{-1} assigned to the COO^- group, and at 1731 cm^{-1} (◆) to COOH group, indicated that CMC is present in the composite scaffold.

The XRD patterns of the novel composite scaffolds and pure CMC synthesized in our laboratory are shown in Figure 4(A,B), respectively. The diffractogram of composite scaffolds demonstrated that the calcium-phosphates consisted of crystalline HA [Fig. 4(A)]. Figure 4(B) shows that CMC is essentially amorphous.

From μ-CT, it can be seen that the porosity of the scaffolds extends from the top to the bottom (black arrows), showing the high interconnectivity of the scaffolds [Fig. 5(A,B)]. On the other hand, the 2D morphometric analysis demonstrated that in average the scaffolds consisted of 24% HA and 76% CMC [Fig. 5(C)]. It was also possible to determine that the composite scaffolds possess 58.9% ± 6% porosity.

Figure 6 shows the profile of the water-uptake capability and weight loss of the composite scaffolds after soaking in a PBS solution for 1 up to 30 days. The results showed a dramatic increase in water absorption in the first hours after immersion in PBS (480%) solution. This trend can be seen until day 7 and after this period a slight stabilization around the day 15 occured [Fig. 6(A)]. After this period of time, it was possible to observe a slight decrease of the

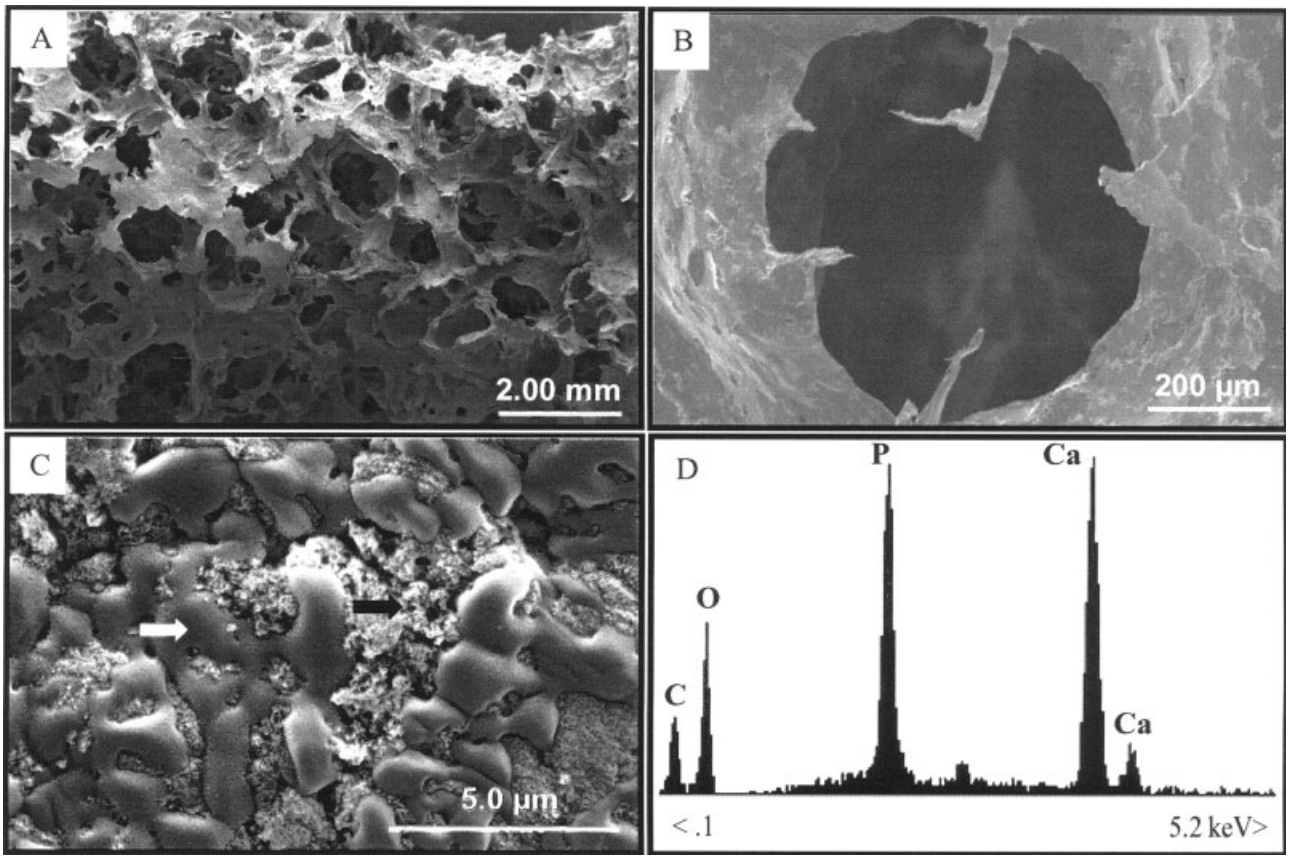

Figure 2. SEM micrographs of the hydroxyapatite/carboxymethylchitosan composite scaffolds: lateral view (A), typical pore (B), interface between the HA and CMC (C), and respective EDS (D).

water-uptake. In respect to the weight loss, a decrease of 3.5% in mass can be seen around day 7. From day 7 until day 15, it is possible to observe a dramatic increase in weight loss (~9% in mass). This trend was observed until day 30 [Fig. 6(B)].

The mechanical properties of the composite scaffolds were assessed using compression tests in dry state. A modulus (E) of 57.3 ± 7 MPa and maximum percentage strength of 51.0 ± 6 MPa was obtained. Additionally, we also carried out studies in wet state by measuring the "push-out" force (Fig. 7) after soaking the composite scaffolds into a PBS solution for the period of 24 hours. A modulus (E) of 0.5 ± 0.3 MPa was calculated by linear regression.

The SEM studies revealed that deposition of aggregates occur after soaking 1 day in a SBF solution [Fig. 8(A)]. From Figure 8(B), it is possible to observe that the surface of the composite scaffolds was completely covered with a thick film with a typical apatite-like morphology, after 7 days.

Figure 9 shows the variation of calcium and phosphorus ion concentrations in the SBF solution after soaking the composite scaffolds for 1–30 days. It is possible to observe that both calcium and phosphorus concentration decreased from day 1 until day 15. In the period of time between day 15 and day 21, an increase of Ca concentration in solution was observed.

DISCUSSION

We demonstrated that CMC can react with $CaCl_2$ in two different autocatalytic electroless media containing Pd^{2+}, namely the acid and oxidant baths, resulting in the formation of opaque dispersions.[48] By performing a potentiometric titration, it was pos-

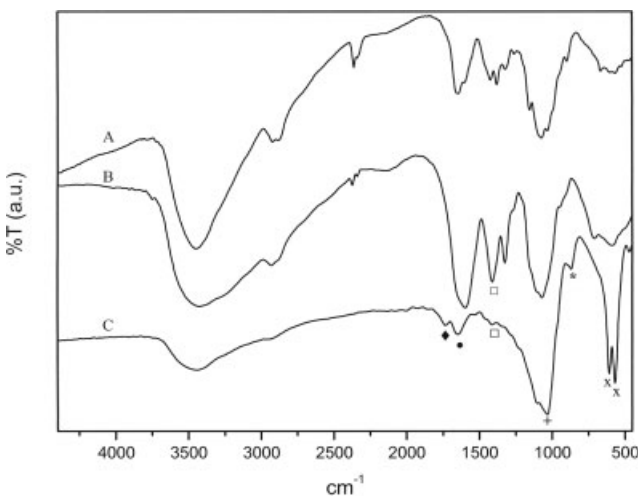

Figure 3. FTIR spectra of: chitosan (A), CMC (B), and hydroxyapatite/carboxymethylchitosan composite scaffolds (C).

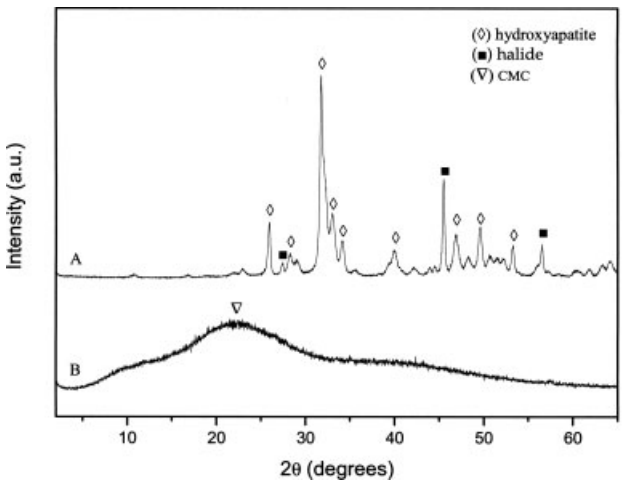

Figure 4. XRD patterns of powders of: hydroxyapatite/carboxymethylchitosan composite scaffolds (A) and CMC (B).

sible to verify that CMC precipitation occurred preferentially in the range of pH's between ~2 and 6 (data not shown). In the same report, we conclude that CMC can coprecipitate with calcium-phosphates to a higher extent when using an acidic bath. This observation may be due to a more effective complexation of CMC with Pd^{2+} ions. By using this method, we were able to produce a composite material which is expected to possess improved mechanical and bioactive behavior.

In the present investigation, SEM studies have shown the existence of two phases on the composite scaffolds, an organic and the inorganic one [Fig. 2(C)]. The EDS analysis showed that the inorganic phase consisted of calcium and phosphorus [Fig. 2(D)]. Therefore, the precipitation of CMC enclosed the calcium phosphate particles inside the polymer. Using a wax spheres leaching method it was possible to develop 3D-macroporous structures with tailored porosity and interconnectivity [Fig. 2(A,B)]. The average pore size was found to be between 20 and 500 μm. Regarding material porosity, Karageorgiou and Kaplan[13] have shown that the range of pore size observed in the composite scaffolds will be beneficial for the cells or tissue ingrowths, and formation of capillaries.

It has been reported[57] that the chelation of Ca^{2+} by the water soluble CMC involves both carboxymethyl group and the 3-OH of a neighboring residue. From these findings, it is expected that the efficiency of CMC on the Pd^{2+}/Ca^{2+} chelation would be dependent not only on the state of protonation of its carboxymethyl groups but also on the degree of substitution, that is percentage of carboxymethyl groups. Therefore, the degree of substitution of CMC will dictate the number of chelation sites. These findings are extremely important because by either changing the pH of the precipitation bath and the initial degree of substituion of CMC or even the molecular weight,[58] we may be able to tailor the chemical composition of the composite scaffolds, that is the efficiency of calcium-phosphate coprecipitation, and ultimately its physicochemical properties.

Another advantage of using CMC on the development of composite scaffolds for bone tissue applications, arises from the fact that CMC allows incorporation of a larger variety of molecules (e.g., bovine serum albumin or bone morphogenetic proteins, BMPs) from precipitating media. But more importantly, this can be done in a wider range of pHs, which it is not possible when using chitosan, for example.[59] We firmly believe that the method proposed herein is a feasible route to incorporate different pH-sensitive proteins in the bulk of the composite scaffolds without any detriment for its activity.

Structural changes of chitosan and its derivatives were assessed by FTIR spectroscopy (Fig. 3). The overlaid IR spectra show that CMC has been successfully synthesized from chitosan. In the region of 3600–3000 cm^{-1} the chitosan, CMC, and composite scaffolds exhibit a highly convoluted IR band because of the various OH stretching contributions. The presence of characteristic absorption bands assigned to the asymmetric (as) and symmetric (s) stretching modes COO^- group at 1593 and 1417 cm^{-1} revealed that carboxymethylation was effective [Fig. 3(A,B)]. Previous studies have shown that CMC possess a substitution degree (DS) of 47% (data not shown). By its turn, the FTIR spectrum of the composite scaffolds exhibited all the characteristic peaks of apatite, that is the presence of phosphate absorption bands, PO_4^{3-} (ν3) at 1190–1020 cm^{-1}, and the PO_4^{3-} (ν4) bands at 601 and 565 cm^{-1} [Fig. 3(C)]. In the composite material, the appearance of a small band at 1417 cm^{-1} attributed to the carboxylic band, and indicate that CMC is also present. The band observed at 1731 cm^{-1} is also attributed to the —COOH group from CMC. Additionally, it was also noted that the peaks corresponding to the carbonate groups, namely at 875 cm^{-1}, attributed to carbonate ν2 and at 1650–1300 cm^{-1}, assigned to carbonate ν3, which can be indicative of the carbonate ion substitution. The presence of the carbonate ν2 and ν3 vibrational modes in the apatites may contribute to a decrease in the hydroxyl band, as seen in the FTIR spectra. It is known that the ν2 sites occur competitively between the OH^- and carbonate groups at the interface of growing crystal, whereas the ν3 sites depend on the competition between phosphate and carbonate ions.

XRD analysis was conducted to investigate the phase content and crystallinity of the developed composite scaffolds. The XRD pattern of the composite scaffolds clearly demonstrated that the calcium phosphate peaks perfectly matched with the standard file for HA [JCPDS 9–432; Fig. 4(A)]. The wide

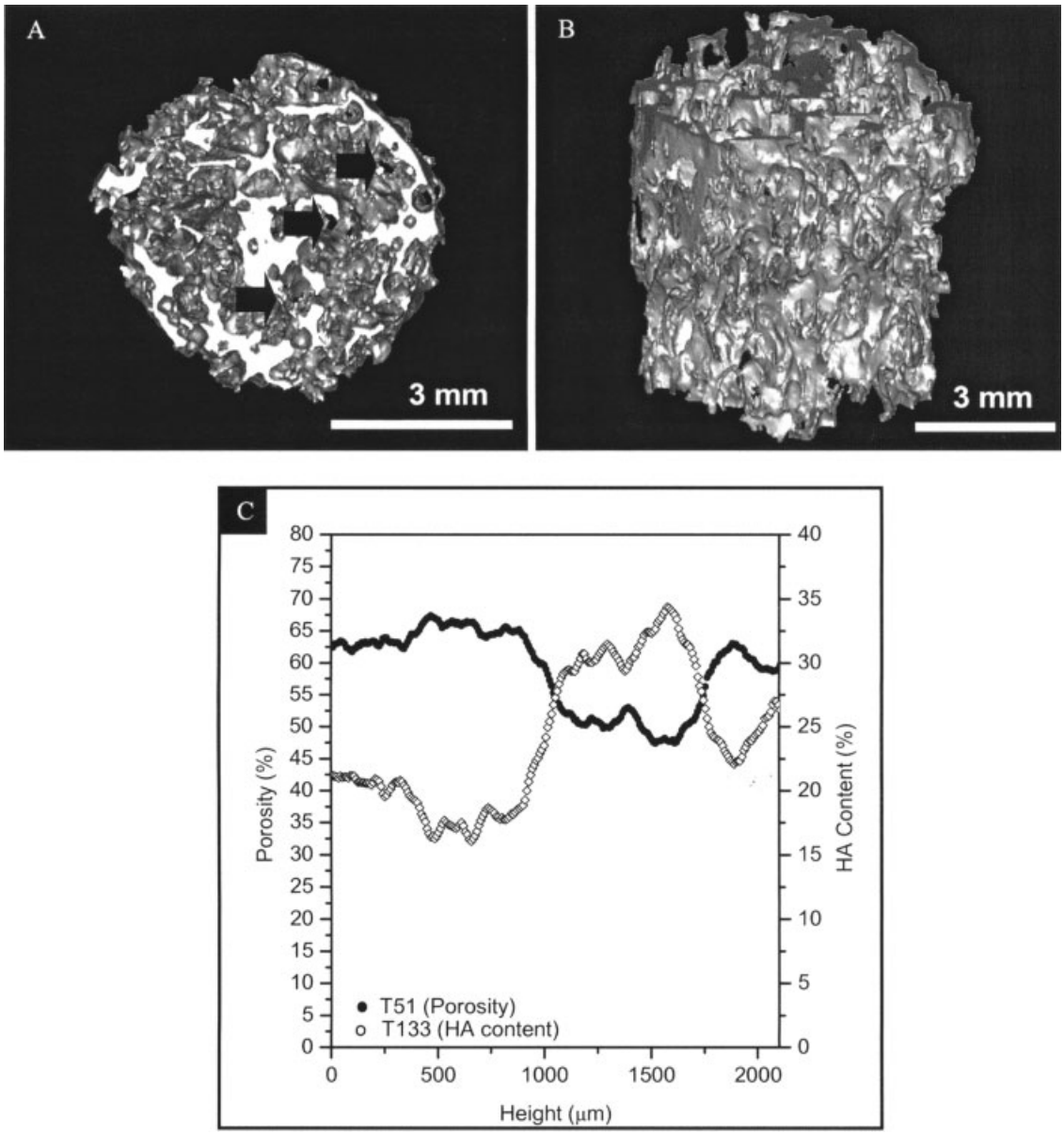

Figure 5. μ-CT of hydroxyapatite/carboxymethylchitosan composite scaffolds: top view (A), lateral view (B), and the respective 2D morphometric analysis (C).

peak appearing approximately at 22° was assigned to CMC [Fig. 4(B)]. Therefore, the carbonate ions detected by FTIR are assigned to surface ones, rather than to carbonate ions in the lattice of phosphate ions. It is also possible to detect the presence of halide in the composite scaffolds, which can be due to the possibility of chemisorption of Pd^{2+} on the surface CMC, as initially hypothesized. Therefore, this data is an indication that CMC is able to bind Pd^{2+}, which in turn may promote the calcium phosphate precipitation. Besides being possible to control the CMC precipitation, this data seems to corroborate previous results, i.e. showed that certain acidic autocatalytic electroless baths allow the control of the Ca and P composition of composite, and the crystallinity of the inorganic phase.[53]

By performing the μ-CT analysis of the novel composite scaffolds we were able to evaluate the porosity, both qualitative and quantitatively (Fig. 5). Composite scaffolds showed a high pore interconnectivity. Applying a threshold 133 (T133), it was possible to determine that in average the scaffolds consisted of 24% HA and 76% CMC. When using the threshold 51 (T51), it was possible to calculate the porosity across the composite scaffolds. This study has shown that composite scaffolds have a porosity of 58.9% ± 6%, on average. It is also possible to observe that the scaffold porosity decreases when the HA content increases. The reason for this observation and for the high interval of porosity may be due to the sedimentation of the HA particles and wax spheres during the drying process. This can be prevented by agitat-

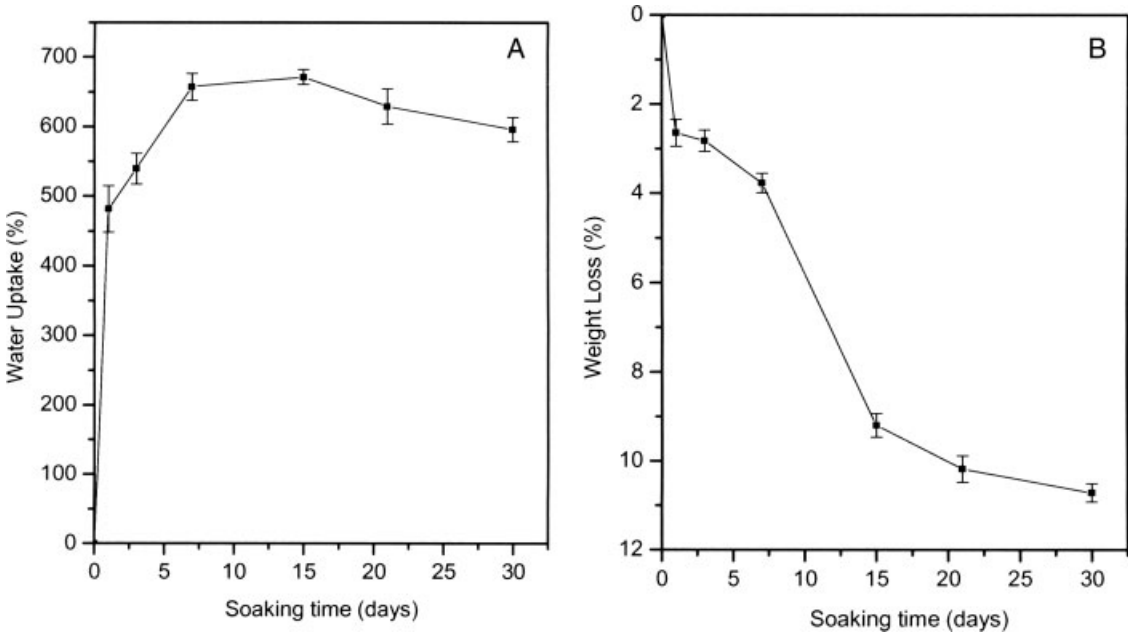

Figure 6. Hydroxyapatite/carboxymethylchitosan composite scaffolds after soaking in PBS solution for times ranging from 1 up to 30 days: water-uptake (A) and weight loss (B).

ing the molds during the preparation of the composite scaffolds. From these results, it can be seen that the developed composite scaffolds have an appropriate porosity to be used as bone substitutes. The method proposed herein presents an important advantage. Porosity and interconnectivity may be easily tailored by varying the content and granulometry of wax spheres.

Biodegradability or bioadsorbability[60] of the 3D substrate is also an essential characteristic in TE applications. Since CMC is a water soluble polymer, we carried out *in vitro* tests to determine the water-uptake capability (swelling) and weight loss of the developed composite scaffolds. The swelling profile showed a dramatic absorption of water (480%) from initial time period until day 7. This swelling behavior is often characteristic of a hydrogel. Nevertheless, it has been reported that CMC swelling is dependent on the pH of the media.[43] Because CMC contains both carboxyl and amino groups, it is possible to control the swelling of the composite scaffolds by loading them with different proteins at different extents, for example. It has been reported that CMC swell at low pH (<2.0) and at pH in the range of 4.0–13.0 because of the protonated amino groups and unprotonated carboxyl groups, respectively.[43] The swelling behavior of CMC is affected by both degree of deacetylation and degree of substitution. The charge of the composite scaffolds can be altered due to the possibility of CMC to bind Ca^{2+} or Pd^{2+}, thus their swelling behavior is expected to be different from the typical CMC gels.

In respect to the weight loss it was possible to observe that composite scaffolds were stable until day 7. After 30 days, a dramatic weight loss occurred (~11% in mass). These results are in agreement with previous results,[43] and can be explained by the water-soluble behavior of CMC. The slight decrease in the swelling of the composite scaffolds after day 15 until day 30 may be a consequence of this dissolution behavior. Chen et al.[43] reported that carboxymethylchitin lose greater than 80% in weight after 20 days of immersion in a phosphate buffer at pH 7.4. The lower weight loss of the novel composite scaffolds suggests that this trend may be a consequence

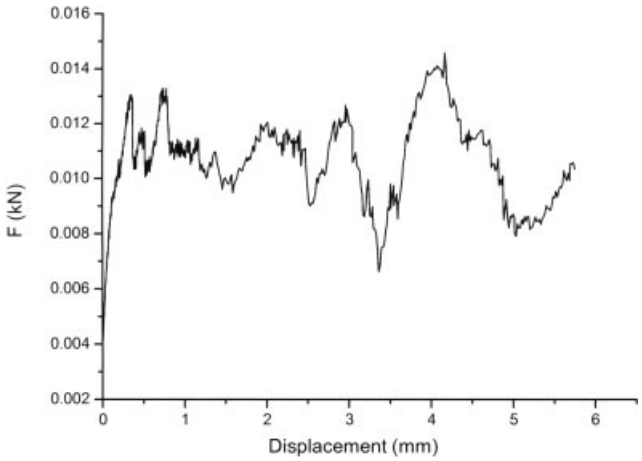

Figure 7. Push-out curve for the hydroxyapatite/carboxymethylchitosan composite scaffolds after soaking in a PBS solution for 24 hours.

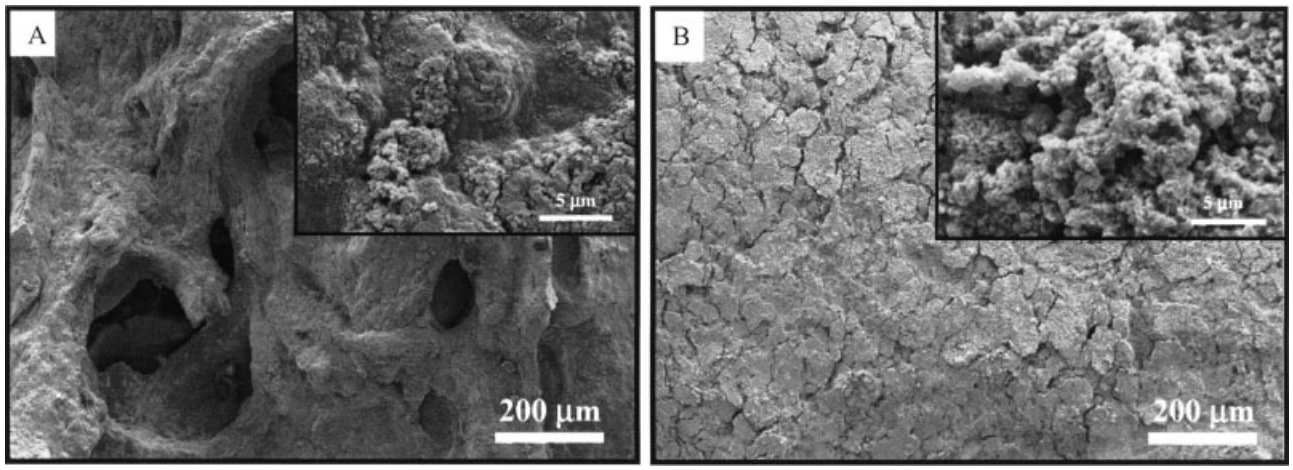

Figure 8. SEM micrographs hydroxyapatite/carboxymethylchitosan composite scaffolds surface after soaking in SBF: 1 day (A) and 7 days (B).

of Ca^{2+} or Pd^{2+} ions chelation, resulting in the development of scaffolds more resistant to dissolution. In this context, future work will be carried out to evaluate the effect of Ca^{2+} or Pd^{2+} binding on the CMC swelling and dissolution behavior. A well-known strategy to control the swelling of the polymers consists in performing the cross-linking.[61] In this context, after coprecipitation of CMC and HA, one may use cross-linking agents, such as silane-coupling agents. This strategy may allow control of the swelling and pH-sensitivity of the composite scaffolds, and may improve the stability of the organic–inorganic network.

The mechanical properties of the composite scaffolds were assessed using compression tests in dry state. A modulus of 57.3 ± 7 MPa and maximum percentage strength of 51.0 ± 6 MPa at ~59% of macroporosity was obtained. Because of the high water-uptake capability of the composite scaffolds, its mechanical properties decrease dramatically after soaking in a PBS solution for 24 hours. While mechanical strength of the composite scaffolds decreased after soaking in PBS solution, the ductibility increased. These tests were carried out in confined cavities to mimic as much as possible the *in vivo* circumstances. At the implantation site the scaffold will be constrained by the bone compression. Interestingly, after undergoing the mechanical solicitation, the composite scaffolds showed a sponge-like behavior. They were capable of recovering the initial shape without fracturing, thus keeping the scaffolds integrity. On the basis of these findings, the moldability of the composite scaffolds can be a major advantage considering that the current orthopedic implant materials, such as sintered HA, are used in a hard form, that requires the surgeon to fit the surgical site around the implant or the need of a material of a desired shape.[30]

Other important parameters have to be considered when developing a TE scaffold. The scaffold must be capable of drug loading and releasing in a controlled manner. In this context, Chen et al.[43] described a reliable methodology to load CMC-based polyampholyte hydrogels with drugs by taking advantage of the high swelling behavior. Because of composite scaffolds mechanical stability in wet state and ability to form hydrogels, the authors believe that the composite scaffolds have great advantages over other materials, because they possess a lower dissolution behavior when compared with CMC alone.

In this study, bioactivty tests were also carried out. These tests showed that deposition of apatite occurs after soaking 1 day in a SBF solution. A thick film covering the surface of the composite scaffolds

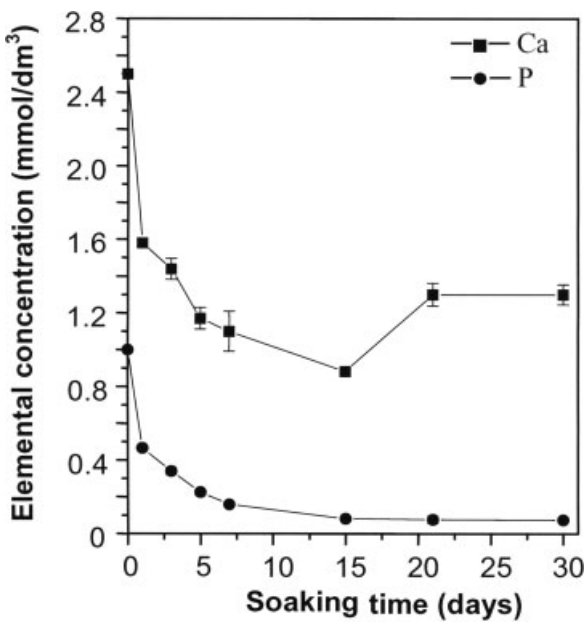

Figure 9. Profile of Ca and P ions in the SBF solution after soaking the hydroxyapatite/carboxymethylchitosan composite scaffolds from 1 up to 30 days.

was observed after 7 days. This bioactive behavior may be explained by the presence of HA in the composite scaffold, which is known to accelerate the formation of bone-like apatite on the surface of implants.[62] The variation of calcium and phosphorus ion in SBF solution was monitored by ICP. From Figure 9 it can be seen that both calcium and phosphorus concentrations decreased from day 1 until day 15. This trend may be a consequence of the consumption of both calcium and phosphorus during the precipitation of the apatite layer on the surface of the composite scaffolds (Fig. 8). The increase of the Ca concentration (from day 15 until day 21) may be a result of CMC dissolution. Since phosphate concentration remained constant, the release of calcium into the SBF solution can only be explained by the release of calcium chelated to CMC, and is not due to a redissolution phenomena. This result is in agreement with the weight loss profile. Further studies are required to elucidate the fast decrease of calcium and phosphorus in the SBF solution.

CONCLUSIONS

This work demonstrated that it is possible to prepare HA/CMC composite scaffolds by combining a novel acidic autocatalytic coprecipitation route and a novel wax spheres leaching methodology. The physicochemical properties of the composite scaffolds may be tailored. This pertains especially to the 3D architecture, content in organic–inorganic phases, and dissolution behavior. These composite scaffolds are very promising whenever degradability and bioactivity are simultaneously desired, as in the case of bone tissue-engineering scaffolding applications. The novel composite scaffolds can possibly improve the incorporation of pH-sensitive proteins up to physiological pH, which is known to be one major drawback of chitosan materials for these types of applications. Future work will be performed to study cell adhesion, proliferation, and to screen the cytotoxicity on the surface of the novel HA/CMC composite scaffolds.

The authors thank Materialise (Belgium) for the MIMICS® software provided to us and LBI (Vienna, Austria) for the μ-CT scans under the scope of HIPPOCRATES project. This work was carried out under the scope of the European NoE EXPERTISSUES (NMP3-CT-2004-500283). The authors also thank Mr. António Sousa Azevedo for his technical assistance in the X-ray diffraction analysis.

References

1. Vacanti JP, Langer R. Tissue engineering: The design and fabrication of living replacement devices for surgical reconstruction and transplantation. Lancet 1999;354:SI32–SI34.
2. Langer R, Vacanti J. Tissue Engineering. Science 1993;260: 920–926.
3. Ohgushi H, Kotobuki N, Funaoka H, Machida H, Hirose M, Tanaka Y, Takakura Y. Tissue engineered ceramic artificial joint—ex vivo osteogenic differentiation of patient mesenchymal cells on total ankle joints for treatment of osteoarthritis. Biomaterials 2005;26:4654–4661.
4. Peterson L, Brittberg M, Kiviranta I, Åkerlund EL, Lindahl A. Autologous chondrocyte transplantation: Biomechanics and long-term durability. Am J Sports Med 2002;30:2–12.
5. Cancedda R, Dozin B, Giannoni P, Quarto R. Tissue engineering and cell therapy of cartilage and bone. Matrix Biol 2003; 22:81–91.
6. Schliephake H, Knebel JW, Aufderheide M, Tauscher M. Use of cultivated osteoprogenitor cells to increase bone formation in segmental mandibular defects: An experimental pilot study in sheep. Int J Oral Maxillofac Surg 2001;30:531.
7. Long MW, Robinson JA, Ashcraft EA, Mann KG. Regulation of human bone marrow-derived osteoprogenitor cells by osteogenic growth factors. J Clin Invest 1995;95:881–887.
8. Holland TA, Tessmar JKV, Tabata Y, Mikos AG. Transforming growth factor-beta 1 release from oligo(poly(ethylene glycol) fumarate) hydrogels in conditions that model the cartilage wound healing environment. J Controlled Release 2004; 94:101–104.
9. Ono I, Yamashita T, Jin H-Y, Ito Y, Hamada H, Akasaka Y, Nakasu M, Ogawa T, Jimbow K. Combination of porous hydroxyapatite and cationic liposomes as a vector for BMP-2 gene therapy. Biomaterials 2004;25:4709.
10. Honda M. Cartilage formation by cultured chondrocytes in a new scaffold made of poly(L-lactide-epsilon-caprolactone) sponge. J Maxillofac Surg 2000;58:767–775.
11. Yamamato M. Promotion of fibrovascular tissue ingrowth into porous sponges by basic fibroblast growth factor. J Mater Sci Mater Med 2000;11:213–218.
12. Ma PX, Langer R. Fabrication of biodegradable polymer foams for cell transplantation and tissue engineering. In: Yarmush M, Morgen J, editors. Tissue Engineering Methods and Protocols. Totowa, NJ: Humana Press; 1998. p 47–56.
13. Karageorgiou V, Kaplan D. Porosity of 3D biomaterial scaffolds and osteogenesis. Biomaterials 2005;26:5474–5491.
14. Tomczok J, Sliwa-Tomczok W, Klein C, Kooten TGv, Kirkpatrick CJ. Biomaterial-induced alterations of human neutrophils under fluid shear stress: Scanning electron microscopical study in vitro. Biomaterials 1996;17:1359–1367.
15. Hutmacher DW. Scaffold design and fabrication technologies for engineering tissues-state of the art and future perspectives. J Biomater Sci Polym Ed 2000;12:107–124.
16. Ma PX. Scaffolds for tissue engineering. Materials Today 2004;7:30–40.
17. Liu X, Ma PX. Polymeric scaffolds for bone tissue engineering. Ann Biomed Eng 2004;32:477–486.
18. Rizzi SC, Heath DJ, Coombes AGA, Bock N, Textor M, Downes S. Biodegradable polymer/hydroxyapatite composites: Surface analysis and initial attachment of human osteoblasts. J Biomed Mater Res 2001;55:475–486.
19. Kawakami T, Antoh M, Hasegawa H, Yamagishi T, Ito M, Eda S. Experimental study on osteoconductive properties of a chitosan-bonded hydroxyapatite self-hardening paste. Biomaterials 1992;13:759–763.
20. Oliveira JM, Rodrigues MT, Silva SS, Malafaya PB, Gomes ME, Viegas CA, Dias IR, Azevedo JT, Mano JF, Reis RL. Novel hydroxyapatite/chitosan bilayered scaffold for osteochondral tissue-engineering applications: Scaffold design and its performance when seeded with goat bone marrow stromal cells. Biomaterials 2006;27:6123.
21. Solchaga LA, Temenoff JS, Gao J, Mikos AG, Caplan AI, Goldberg VM. Repair of osteochondral defects with hyaluronan- and polyester-based scaffolds. Osteoarthritis Cartilage 2005;13:297.

22. Spoerke ED, Murray NG, Li H, Brinson LC, Dunand DC, Stupp SI. A bioactive titanium foam scaffold for bone repair. Acta Biomater 2005;1:523.
23. Turhani D, Cvikl B, Watzinger E, Weißenböck M, Yerit K, Thurnher D, Lauer G, Ewers R. In vitro growth and differentiation of osteoblast-like cells on hydroxyapatite ceramic granule calcified from red algae. J Oral Maxillofac Surg 2005; 63:793–799.
24. Noriko Kotobuki, Koji Ioku, Daisuke Kawagoe, Hirotaka Fujimori, Seishi Goto, Ohgushi H. Observation of osteogenic differentiation cascade of living mesenchymal stem cells on transparent hydroxyapatite ceramics. Biomaterials 2005;26: 779–785.
25. Martino AD, Sittinger M, Makarand VR. Chitosan: A versatile biopolymer for orthopaedic tissue-engineering. Biomaterials 2005;26:5983–5990.
26. Shi C, Zhu Y, Ran X, Wang M, Su Y, Cheng T. Therapeutic potential of chitosan and its derivatives in regenerative medicine. J Surg Res 2006;133:185.
27. Murugan R, Ramakrishna S. Bioresorbable composite bone paste using polysaccharide based nano hydroxyapatite. Biomaterials 2004;25:3829–3835.
28. Ma PX, Zhang RY, Xiao GZ, Franceschi R. Engineering new bone tissue in vitro on highly porous poly(alpha-hydroxyl acids)/hydroxyapatite composite scaffolds. J Biomed Mater Res 2001;54:284–293.
29. Ge Z, Baguenard S, Lim LY, Wee A, Khor E. Hydroxyapatite-chitin materials as potential tissue engineered bone substitutes. Biomaterials 2004;25:1049–1058.
30. Xu HHK, Simon CGS, Jr. Fast setting calcium phosphate-chitosan scaffold: Mechanical properties and biocompatibility. Biomaterials 2005;26:1337–1348.
31. Zhang Y, Zhang M. Microstructural and mechanical characterization of chitosan scaffolds reinforced by calcium phosphates. J Non-Cryst Solids 2001;282:159–164.
32. Wan ACA, Khor E, Hastings GW. Preparation of a chitin-apatite composite by in situ precipitation onto porous chitin scaffolds. J Biomed Mater Res 1998;41:541–548.
33. Ang TH, Sultana FSA, Hutmacher DW, Wong YS, Fuh JYH, Mo XM, Loh HT, Burdet E, Teoh SH. Fabrication of 3D chitosan-hydroxyapatite scaffolds using a robotic dispensing system. Mater Sci Eng C 2002;20:35–42.
34. Kim H-W, Knowles JC, Kim H-E. Hydroxyapatite and gelatin composite foams processed via novel freeze-drying and crosslinking for use as temporary hard tissue scaffolds. J Biomed Mater Res A 2005;72:136–145.
35. Hollinger JO. Strategies for regenerating bone of the craniofacial complex. Bone 1993;14:575–580.
36. Marques AP, Reis RL, Hunt JA. The biocompatibility of novel starch-based polymers and composites: In vitro studies. Biomaterials 2002;23:1471–1478.
37. Sun T, Xu P, Liu Q, Xue J, Xi W. Graft copolymerization of methacrylic acid onto carboxymethylchitosan. Eur Polym J 2003;39:189–192.
38. Muzzarelli R. Carboxymethylated chitins and chitosans. Carbohydr Polym 1988;8:1–21.
39. Ge H-C, Luo D-K. Preparation of carboxymethylchitosan in aqueous solution under microwave irradiation. Carbohydr Res 2005;340:1351–1356.
40. Dobetti L, Delben F. Binding of metal cations by *N*-carboxymethylchitosans in water. Carbohydr Polym. 1992;18:273–282.
41. Delben F, Muzzarelli RAA. Thermodynamic study of the interaction of *N*-carboxymethylchitosan with divalent metal ions. Carbohydr Polym 1989;11:221–232.
42. Chen S-C, Wu Y-C, Mi F-L, Lin Y-H, Yu L-C, Sun H-W. A novel pH-sensitive hydrogel composed of *N*,*O*-carboxymethylchitosan and alginate cross-linked by genipin for protein drug delivery. J Controlled Release 2004;96:285–300.
43. Chen L, Tian Z, Du Y. Synthesis and pH sensitivity of carboxymethyl chitosan-based polyampholyte hydrogels for protein carrier matrices. Biomaterials 2004;25:3725–3732.
44. Zhou J, Elson C, Lee TDG. Reduction in postoperative adhesion formation and re-formation after an abdominal operation with the use of *N*,*O*-carboxymethylchitosan. Surgery 2004; 135:307–312.
45. Liang P, Zhao Y, Shen Q, Wang D, Xu D. The effect of carboxymethylchitosan on the precipitation of calcium carbonate. J Cryst Growth 2004;261:571–576.
46. Muzzarelli RAA, Ramos V, Stanic V, Dubini B, Mattioli-Belmonte M, Tosi G, Giardino R. Osteogenesis promoted by calcium phosphate *N*,*N*-dicarboxymethylchitosan. Carbohydr Polym 1998;36:267–276.
47. Viala S, Freche M, Lacout JL. Effect of chitosan on octacalcium phosphate crystal growth. Carhohydr Polym 1996;29: 197–201.
48. Costa SA, Oliveira JM, Leonor IB, Reis RL. Carboxymethilchitosan/calcium phosphate hybrid materials prepared by an innovative "auto-catalytic" co-precipitation method. Key Eng Mater 2005;284–286:701–704.
49. Leonor IB, Reis RL. An innovative "auto-catalytic" deposition route to produce calcium-phosphate coatings on polymeric biomaterials. J Mater Sci: Mater Med 2003;14:435–441.
50. Touchais-Papet E, Charbonnier M, Romand M. Electroless metallization of carbon substrates. Appl Surf Sci 1999;138/ 139:557.
51. Charbonnier M, Alami M, Romand M, Girardeau-Montaut JP, Afif M. Laser-assisted grafting onto polycarbonate: Application to metallization by chemical means. Appl Surf Sci 1997;109/110:206.
52. Blaser H-U, Indolese A, Schnyder A, Steiner H, Studer M. Supported palladium catalysts for fine chemicals synthesis. J Mol Catal A Chem 2001;173:3.
53. Oliveira JM, Leonor IB, Reis R. Preparation of bioactive coatings on the surface of bioinert polymers through an innovative "auto-catalytic" electroless route. Key Eng Mater 2005; 284–286:203–220.
54. Kokubo T, Kushitani H, Sakka S, Kitsugi T, Yamamuro T. Solutions able to reproduce in vivo surface-structure changes in bioactive glass-ceramic A-W. J Biomed Mater Res 1990;24: 721–734.
55. Chen X-G, Park H-J. Chemical characteristics of *O*-carboxymethylchitosans related to the preparation conditions. Carbohydr Polym 2003;53:355–359.
56. Boesel LF, Mano JF, Reis RL. Optimization of the formulation and mechanical properties of starch based partially degradable bone cements. J Mater Sci Mater Med 2004;15: 73–83.
57. Uraki Y, Fujii Y, Matsuoka T, Miura Y, Tokura S. Site specific binding of calcium ions to anionic chitin derivatives. Carbohydr Polym 1993;20:139–143.
58. Chen X, Wang Z, Liu W, Park H. The effect of carboxymethylchitosan on proliferation and collagen secretion of normal and keloid skin fibroblasts. Biomaterials 2002;23:4609–4614.
59. Chenite A, Buschamann M, Wang D, Chaput C, Kanadani N. Rheological characterisation of thermogelling chitosan/glycerol-phosphate solutions. Carbohydr Res 2001;46:39–47.
60. Hutmacher DW. Scaffolds in tissue engineering bone and cartilage. Biomaterials 2000;21:2529–2543.
61. Berger J, Reist M, Mayer JM, Felt O, Peppas NA, Gurny R. Structure and interactions in covalently and ionically crosslinked chitosan hydrogels for biomedical applications. Eur J Pharm Biopharm 2004;57:19–34.
62. Sabokbar A, Pandey R, Diaz J, Quinn JMW, Murray DW. Hydroxyapatite particles are capable of inducing osteoclast formation. J Mater Sci Mater Med 2001;12:659–664.